Published in final edited form as:

Neuroscience. 2017 October 24; 362: 265–271. doi:10.1016/j.neuroscience.2017.08.048.

Hyper-oligodendrogenesis at the vascular niche and reduced blood-brain barrier integrity in the prefrontal cortex during protracted abstinence

Sucharita S. Somkuwar[1], **McKenzie J. Fannon**[1], **Tran Bao Nguyen**[2], and **Chitra D. Mandyam**[1,2,3,*]

[1]VA San Diego Healthcare System, San Diego, CA, USA

[2]Skaggs School or Pharmacy and Pharmaceutical Sciences, University of California San Diego, CA, USA

[3]Department of Anesthesiology, University of California San Diego, CA, USA

Abstract

Alcoholism is a relapsing disorder with limited treatment options, in part due to our limited understanding of the disease etiology. We have recently shown that increased ethanol-seeking in a behavioral model of relapse in a rat model of alcoholism was associated with increased oligodendrogenesis which was positively correlated with platelet/endothelial cell adhesion molecule (PECAM-1) expression in the medial prefrontal cortex (mPFC). The current study investigated whether newly born oligodendrocytes form close physical associations with endothelial cells expressing PECAM-1 and whether these changes were accompanied by altered blood-brain barrier (BBB) integrity. Colableling and confocal analysis demonstrate that newly born oligodendroglia were always located in close physical proximity to PECAM-1 in the mPFC of rats that were ethanol dependent and demonstrated high propensity for relapse. Notably, the endothelial proximity of new oligodendrocytes was associated with reduced expression of endothelial barrier antigen (SMI-71), a marker for BBB integrity. Furthermore, voluntary wheel running during abstinence enhanced SMI-71 expression in endothelial cells, indicating protection against abstinence-induced reduction in BBB integrity. Taken together, these results suggest that ethanol experience and abstinence disrupts homeostasis in the oligo-vascular niche in the mPFC. Reversing these mechanisms may hold the key to reducing propensity for relapse in individuals with moderate to severe alcohol use disorder.

Keywords

BrdU; PECAM-1; Blood-brain barrier; SMI-71; ethanol; self-administration

*Correspondence: Chitra D. Mandyam, Ph.D., VA San Diego Healthcare System, 3350 La Jolla Village Dr, San Diego, CA 92161, USA; Tel: (858) 552-8585 Ext 5972; cmandyam@scripps.edu.

The authors have no conflicts of interest to report.

Introduction

Chronic intermittent ethanol vapor inhalation (CIE) procedure is a widely accepted model for moderate to severe alcohol use disorder (AUD; (Gilpin *et al.*, 2008; Vendruscolo & Roberts, 2014). This model is invaluable for identifying the circuitry and neurochemistry underlying the reward-deficient and stress-surfeit characteristics of addiction (Koob & Volkow, 2010); however the addiction pathology extends beyond adaptations in neurocircuitry into processes such as inflammation and gliosis (Coller & Hutchinson, 2012; Somkuwar *et al.*, 2014). In fact, neuronal damage in AUD has been ascribed, in part, to the concerted feed-forward interaction between blood-brain barrier (BBB) damage and neuroinflammation (Haorah *et al.*, 2007; Privratsky *et al.*, 2010; Alikunju *et al.*, 2011). Thus, understanding ethanol-induced disruptions in function of cerebral endothelium and other non-neuronal cells may help elucidate AUD neuropathology.

The current study explores the role of the oligovascular niche (Arai & Lo, 2009) in AUD. Disrupted oligodendroglial homeostasis in the medial prefrontal cortex (mPFC) was associated with escalated ethanol intake in CIE rats (Richardson *et al.*, 2009; Somkuwar *et al.*, 2015). Specifically, high ethanol intake was shown to reduce proliferation of stem-like cells in several areas of the adult rodent brain, including mPFC (Nixon & Crews, 2002; Crews & Nixon, 2009; Richardson *et al.*, 2009; Hansson *et al.*, 2010). During early ethanol abstinence (3-7 days), compensatory hyperproliferation of stem cells was observed in several brain regions (Nixon & Crews, 2004; Hansson *et al.*, 2010), including the mPFC (Somkuwar *et al.*, 2015). These newly born neural cells in the mPFC survived and differentiated, primarily (>85%) into new oligodendrocytes (Somkuwar *et al.*, 2015). This increased/rebound oligodendrogenesis was associated with increased ethanol drinking (Somkuwar *et al.*, 2015), increased ethanol seeking and decreased neuronal activation as measured by Fos expression in the mPFC after prolonged abstinence (Somkuwar *et al.*, 2016). Voluntary wheel running (WR) during prolonged abstinence did not alter ethanol drinking, but inhibited ethanol seeking, increased mPFC neuronal activation and rescued mPFC oligodendroglial homeostasis (Somkuwar *et al.*, 2016). Since oligodendroglial turnover and maturation depends on cerebrovascular health (Arai & Lo, 2009; Miyamoto *et al.*, 2014; Maki *et al.*, 2015), it was not surprising that a cerebral endothelial marker, platelet/endothelial cell adhesion molecule-1 (PECAM-1 or CD-31), was also increased in association with the increased ethanol seeking, and these alterations were reduced by wheel running (Somkuwar *et al.*, 2016). However, it is unclear whether the oligodendroglial hyperproliferation is connected functionally to compromised cerebrovascular health in this model of AUD.

We hypothesized that (1) protracted abstinence from ethanol enhances oligodendrocytes within close proximity to vasculature, (2) the enhanced oligodendroglial-vascular proximity is associated with reduced BBB integrity, and (3) wheel running during abstinence will prevent these alterations. The mPFC tissue from rats previously found to exhibit enhanced oligodendrogenesis and increased ethanol seeking after prolonged abstinence (Somkuwar *et al.*, 2016) was used for the current study. The relative localization of PECAM-1 and the newly born oligodendrocyte was conducted to understand the anatomical relation between

the damaged endothelium and oligodendrogenesis. BBB integrity was investigated using immunohistochemical analysis of endothelial barrier antigen (EBA or SMI-71). For example, studies conducted in adult rats in models of neuroinflammation and spinal cord injury have demonstrated that SMI-71 expression in the brain and spinal cord negatively correlated with infiltrated evans blue (EB) dye, suggesting that a reduction in SMI-71 expression shows enhanced BBB permeability and reduced BBB integrity (Matsushita *et al.*, 2015; Park *et al.*, 2015). Animal models of dyskinesia in adult rats also demonstrate a negative association between albumin immunostaining in the neuropil (measure of dysfunctional BBB) and SMI-71 immunostaining in the brain, supporting the previous findings that SMI-71 expression decreases with enhanced dysfunctional BBB (Westin *et al.*, 2006). Furthermore, a direct support for SMI-71 as a measure for vascular damage, and hence BBB integrity, comes from toxin-induced studies in adult rats, where microvascular damage induced by *clostridium perfringens* type D epsilon toxin reduced SMI-71 immunostaining (Finnie *et al.*, 2014). SMI-71 is expressed on the luminal side of endothelial cells only in areas with a selectively permeable BBB (Sternberger & Sternberger, 1987). Under pathological conditions that disrupt BBB function and increase BBB permeability, such as cerebral ischemia (Pelz *et al.*, 2013), rarefaction of SMI-71 expression is expected.

Material/Methods

Prefrontal cortical tissue from forty-nine adult male Wistar rats (Charles River) were used for the study. All experimental procedures were carried out in strict adherence to the National Institutes of Health Guide for the Care and Use of Laboratory Animals (NIH publication number 85–23, revised 1996), and were approved by the Institutional Animal Care and Use Committee at The Scripps Research Institute.

Effects of history of ethanol experience and access to running wheel during ethanol abstinence on the oligo-vascular homeostasis in the mPFC was investigated to provide potential mechanistic link between the behavioral protection against ethanol seeking and the neuro-adaptive effects of wheel running during abstinence (Somkuwar *et al.*, 2016). The experimental design is presented schematically (Figure 1). Briefly, adult male Wistar rats were trained to self-administer ethanol (10% v/v in water) using operant conditioning. The rats were divided into two groups; one received ethanol vapors in a 14hON/10hOFF CIE schedule (CIE-ED; n=17) for a period of seven weeks to develop moderate to severe AUD (Gilpin *et al.*, 2008). The other group did not receive ethanol vapor, however, self-administered ethanol (ED; n=20). Ethanol self-administration in these rats was reported previously; while CIE-ED escalated ethanol drinking, ED maintained low ethanol intake over weeks (Somkuwar *et al.*, 2016). After week 7, all ethanol access was removed and ethanol abstinence was maintained under either standard housing conditions (CIE-ED; n=8 and ED; n=8) or with *ad libitum* home-cage wheel access (CIE-ED-WR; n=9 and ED-WR; n=12). An additional cohort of age-matched rats with regular housing conditions (ethanol and wheel naïve; Naive, n=6), and with wheel access (WR, n=6) were maintained for the same duration as the rats with ethanol history. After 3 days of abstinence, all rats were administered an exogenous marker of cell division, 5′-bromo-2-deoxyuridine (BrdU; 150 mg/kg, i.p.) to label proliferating cells (Dayer *et al.*, 2003; Mandyam *et al.*, 2007; Taupin, 2007). After 20 days of abstinence, ED, CIE-ED, ED-WR and CIE-ED-WR rats were

subjected to one session of ethanol self-administration, six sessions of extinction training, and one session of cued-context induced reinstatement of ethanol-seeking behavior. For extinction sessions, operant boxes different from those used for self-administration were used and the house-light and white noise were turned on, and no cue-lights were available following lever presses. Finally lever response did not result in the delivery of ethanol. Both lever responses were recorded. After 6 days of extinction, rats were subjected to one session of cued-context reinstatement of ethanol seeking. Specifically, rats were introduced to operant chambers under conditions identical to training and maintenance (no house-light, no white noise; operant boxes used for self-administration). Active lever responses resulted in the presentation of the cue-light for 4 sec, but did not result in the delivery of ethanol. Both active and inactive lever responses were recorded. The self-administration behavior and wheel running activity for these rats have been published previously (Somkuwar *et al.*, 2016). Two-hours after the reinstatement session, all rats were euthanized and their brain were post-fixed in 4% paraformaldehyde for immunohistochemistry.

Brain tissue was sliced in 40μm sections along the coronal plane on a freezing microtome. Every ninth section through the PFC (+3.7 to +2.5 mm from bregma; 4 sections per rat) was mounted on Superfrost® Plus slides and dried overnight and used for BrdU analysis. Quantitative immunohistochemical assay performed using a previously published optical fractionator method (Kim *et al.*, 2015); the sections were counter-stained with Vector Fast Red (a nuclear stain). The quantitative data for BrdU has been previously reported (Somkuwar *et al.*, 2016). To determine the phenotype of BrdU labeled cells colabeling of BrdU (Abcam) was performed with the transcription factor Olig2 (gift from Dr. Charles Stiles), followed by biotinylated secondary and fluorescent labeling via tyramide signal amplification. The percent of BrdU cells colabeled with Olig2 were determined and the number of BrdU/Olig2 labeled cells were computed. These values were compared between groups using 2-way ANOVA (wheel access, 2 levels and ethanol history, 3 levels); significant interaction and/or main effects were further investigated using Holm-Sidak's post-hoc analysis.

A separate set of coronal sections of the brain (+3.0 to +3.7mm from bregma) were immunoprobed for quantifying the spatial distribution of newly born oligodendrocytes (BrdU) relative to cerebral endothelium (PECAM-1). To determine the distribution of newly born oligodendroglia, mPFC sections were immunoprobed for both BrdU and PECAM-1 (gift from Dr. Peter Newman), followed by biotinylated secondary and fluorescent labeling via tyramide signal amplification. Confocal analysis was conducted with Zeiss Axiovert 100M (Kim & Mandyam, 2014; Kim *et al.,* 2014; Somkuwar *et al.,* 2015). Note, PECAM-1 expression is not contingent on the functional integrity of endothelium (for review, (Newman, 1994)). The proximity between surviving BrdU cells and the nearest PECAM-1 labeled cell was measured using the “linear scale” function on a Zeiss AxioImager equipped with the software LSM510. Percentage of BrdU cells that were juxtaposed (physical touching with PECAM-1 cell), proximal (<5 μm apart from PECAM-1 cell), intermediate (between 5 μm and 30 μm apart from PECAM-1 cell) and distal (>30 μm apart from PECAM-1 cell) were calculated for each rat (5-40 cells/rat). Further, the number of BrdU cells within each location was calculated from the total number of BrdU cells obtained across mPFC (+2.6 to +4.5mm from bregma, 4 sections/rat) using quantitative

immunohistochemical analysis (Somkuwar *et al.*, 2016). Fraction and number of BrdU cells were analyzed using 3-way repeated-measures ANOVA with wheel access (2 levels) and ethanol history (3 levels) as between-subjects and distance (4 levels) as within-subjects independent variables. Huyhn-Feldt correction was applied to adjust for the violation of the sphericity hypothesis (i.e. the error covariance matrix of the orthonomalized transformed dependent variables is proportional to an identity matrix; Mauchly's test) for repeated-measures ANOVA. Significant effects at specific localization levels were further probed using 2-way ANOVAs (wheel access, 2 levels and ethanol history, 3 levels) and Sidak's post-hoc analyses.

Coronal sections (+3.0 to +3.7mm from bregma, 1 section/rat) were immunoprobed for SMI-71 (or EBA, 1:500, rat polyclonal), and biotin-tagged secondary antibodies and then visualized with DAB. Colored, white-balanced images were captured with StereoInvestigator software (MicroBrightField); and DAB levels (% area stained) in the infralimbic, prelimbic cortex and cingulate gyrus regions were evaluated using ImageJ software (NIH). Average area stained across the three mPFC subregions was compared between groups using 2-way ANOVA (wheel access, 2 levels and ethanol history, 3 levels) followed by Holm-Sidak's post-hoc analysis.

Results

The number of BrdU/Olig2 cells were enhanced by ethanol treatment. Two-way ANOVA revealed a significant ethanol treatment × wheel running interaction ($F_{EthanolHistory \times WheelAccess}[2, 34] = 20.76$, $p<0.001$), main effect of ethanol treatment ($F_{EthanolHistory}[2, 34] = 30.96$, $p<0.001$), and main effect of wheel running ($F_{WheelAccess}[1, 34] = 74.55$, $p<0.001$). Post hoc analysis demonstrated higher number of BrdU/Olig2 cells in ED and CIE-ED rats compared with sedentary controls ($p<0.01$), and lower number of BrdU/Olig2 cells in ED-WR and CIE-ED-WR rats compared to non-wheel groups ($p<0.01$; Figure 2a). Co-labeling analysis revealed no significant differences between the ratio of BrdU cells expressing Olig2 between any of the experimental groups, and there was greater than 95% co-labeling in all the groups (data not shown).

Analysis revealed that the distribution of surviving BrdU cells in relation to PECAM-1 expression showed intermediate>proximal>distal=juxtaposed ($F_{Distance}[3,120]=34.6$, $p<0.0001$; Figure 3a-b). However, percent of juxtaposed, proximal, intermediate and distal BrdU cells relative to PECAM-1 immunofluorescence was not different between wheel access and ethanol history groups (data not shown). Analysis of number of cells in these localizations reveled significant interactions of distance and ethanol history ($F_{Distance \times EthanolHistory}[3,120]=3.62$, $p=0.010$) and distance and wheel access ($F_{Distance \times WheelAccess}[3,120]=3.25$, $p=0.028$), but not for 3-way interaction ($F_{Distance \times EthanolHistory \times WheelAccess}[3,120]=1.76$, $p=0.121$). Further investigation into individual levels of localization revealed a difference between low and high ethanol intake histories only in the juxtaposed fraction, i.e. in the 14.5% of the surviving BrdU cells (Figure 3b-c). Specifically, significant main effects of wheel access, ethanol history and their interaction were found ($F_{WheelAccess}[1,40]=4.52$, $p=0.040$; $F_{EthanolHistory}[2,40]=4.95$, $p=0.012$; $F_{EthanolHistory \times WheelAccess}[2,40]=3.93$, $p=0.028$; Figure 3c). Despite the variability

in the CIE-ED group, CIE-ED rats showed greater number of juxtaposed BrdU cells compared to both ED and naïve (ps<0.01), which was reduced by wheel access during abstinence (p<0.005), such that CIE-ED-WR was not different from WR and ED-WR. In contrast, BrdU cells proximal to and at intermediate separation from PECAM-1 were enhanced in both ED and CIE-ED compared to naïve, and this burst was normalized to WR levels in both ED-WR and CIE-ED-WR (data and statistics in Table 1).

SMI-71 expression, expressed as % of area contoured, revealed significant main effect of wheel access and interaction of wheel access and ethanol history ($F_{WheelAccess}[1,42]=18.0$, $p<0.0001$; $F_{EthanolHistory}[2,42]=2.72$, $p=0.077$; $F_{EthanolHistory \times WheelAccess}[2,42]=6.52$, $p=0.003$; Figure 4a-f). Wheel access did not enhance SMI-71 stained area in the ethanol naïve group ($t(0.1)=42, p=0.9$), but it increased SMI-71 stained area in both ED and CIE-ED rats (ED vs ED-WR: $t(2.6)=42$, $p=0.02$; CIE-ED vs CIE-ED-WR: $t(5.5)=42$, $p<0.001$). CIE-ED-WR had greater expression of SMI-71 compared to ED-WR ($t(3.2)=42$, $p=0.006$) and WR ($t(3.99)=42$, $p=0.0008$).

Discussion

The current findings in accordance with our recent report demonstrate that enhanced oligodendrogenesis in the mPFC of ethanol abstinent rats (both ED and CIE-ED) was associated with enhanced ethanol seeking, and wheel running during abstinence reduced both ethanol seeking and oligodendrogenesis (Somkuwar *et al.*, 2016). Our recent report also revealed that PECAM-1 expression (using immunoblotting analysis on mPFC homogenate) was also increased in ethanol abstinent rats, and normalized to control levels in rats with wheel access during abstinence (Somkuwar *et al.*, 2016). Since cerebral endothelial cells promote oligodendrogenesis and vice versa, in part, via exchange of trophic factors (Arai & Lo, 2009; Miyamoto *et al.*, 2014), it was not surprising that PECAM-1 and oligodendroglial proliferation in the mPFC were modulated in tandem during ethanol abstinence (Somkuwar *et al.*, 2016). The major findings reported herein are that prolonged abstinence and reinstatement of ethanol seeking in CIE-ED rats increased oligodendrogenesis within a 30μ radius around the damaged endothelium expressing PECAM-1 and these effects were associated with reduction in SMI-71 expression on endothelial cells. Reduced SMI-71 expression was also observed in ED rats, however, these effects did not correlate with closer proximity of oligodendrocytes with endothelial cells as seen in CIE-ED rats. Our findings of reduced SMI-71 immunostaining in the mPFC in ED and CIE-ED rats demonstrate that protracted abstinence from chronic ethanol experience produces unheralded effects on endothelial cells and BBB integrity that may be associated with dependence-like syndrome.

Chronic ethanol exposure induces oxidative stress and neuroinflammation which may contribute to BBB damage (Haorah *et al.*, 2005; Wang *et al.*, 2013; Hernandez *et al.*, 2016), and to cognitive deficits (Tiwari *et al.*, 2009; Hernandez *et al.*, 2016). In fact, oxidative stress in endothelial cells suppresses release of trophic factors necessary for oligodendrogenesis (Arai & Lo, 2009), which explains the reduced proliferation of oligodendrocyte progenitors in the mPFC observed during CIE (Richardson *et al.*, 2009). Thus, BBB damage noted herein may be an effect of ethanol exposure that persisted into abstinence. As a corollary, the increased PECAM-1 expression and oligodendrogenesis during abstinence could emphasize

physiological mechanisms of recovery from ethanol-induced oxidative damage. However, these effects appear to indicate maladaptive plasticity, such that, they were associated with enhanced cue-induced reinstatement of ethanol seeking, a behavioral paradigm for relapse, and with decreased neuronal activation in the mPFC (Somkuwar *et al.*, 2016), which together suggests reduced executive function and behavioral inhibition (Warthen *et al.*, 2016). A potential limitation of the currently used methodology is that it is not clear whether the observed increase in PECAM-1 expression is due to increases in the number of vascular endothelial cells or increased expression of PECAM-1 protein within the residual vascular endothelial cells. The current findings of reduced SMI-71 on endothelial cells in ED and CIE-ED rats during abstinence suggest that the expression of PECAM-1 within the existing vasculature is increased which may lead to angiogenesis with longer abstinence; however, this hypothesis needs to be validated. Similar increase in PECAM-1 expression and decrease in SMI-71 expression was reported in the basal ganglia of a rodent model of dyskinesia, where an increase in BBB permeability was also observed (Westin *et al.*, 2006), suggesting a pre-angiogenic state in the basal ganglia. Although the current findings do not provide any causation between alterations in PECAM-1 and SMI-71 and relapse to ethanol seeking, and these studies are beyond the scope of the current report, future studies should investigate the functional consequence of enhanced PECAM-1 expression with BBB dysfunction during ethanol abstinence.

Wheel running performed voluntarily during abstinence was protective against cue-triggered ethanol seeking, suggesting a preservation of the response inhibition learned during extinction (Somkuwar *et al.*, 2016), a behavior that is heavily reliant on the mPFC (Lasseter *et al.*, 2010). Wheel running also increased neuronal activation, normalized oligodendrogenesis and PECAM-1 expression (Somkuwar *et al.*, 2016) and increased expression of SMI-71 supporting restoration of a healthy BBB in mPFC (current findings). Exercise has been shown to be BBB protective in other disease models, such as cerebral ischemia and multiple sclerosis (Souza *et al.*, 2016), and to reduce disease progression and restore neuronal function in several other neuropathologies (Phillips *et al.*, 2014). Future studies should investigate the mechanistic link between PECAM-1 and ethanol seeking (via pharmacological and/or genetic manipulation) in the context of hyperproliferation of oligodendrocytes in the mPFC.

An interesting observation in the current study was the lack of difference in SMI-71 expression in mPFC in CIE-ED and ED rats; these effects may be due to floor effect in SMI-71 expression, since the magnitude of SMI-71 recovery following wheel access during alcohol abstinence was greater in CIE-ED-WR compared to ED-WR. Alternatively, the nature of BBB damage may be qualitatively different between CIE-ED and ED rats that could not be harnessed with SMI-71 expression. Notably, only in the CIE-ED rats, increased oligodendrogenesis was observed juxtaposed with the damaged cerebral endothelium. One limitation of this analysis is that PECAM-1-BrdU spatial relation is quantified in tissue slices and not in a more physiologically accurate 3D space. Thus, it is possible that PECAM-1 may be closer to BrdU than apparent here, although that will likely not alter the number of juxtaposed cells. Further, others have noted oligodendrocyte progenitor cells are located close to cerebral endothelia, and under pathological conditions, such as oxidative stress, weaken the endothelial barrier in a paracrine manner (Seo *et al.*, 2013). Thus, one

could predict that in rats with an AUD phenotype, oligodendrocyte progenitor cells contribute to BBB damage and that during abstinence, the impaired BBB provides a conducive environment for maladaptive oligodendrogenesis.

Acknowledgments

The authors thank Dr. Charles Stiles, Harvard Medical School for the Olig2 antibody and Dr. Peter J. Newman, BloodCenter of Wisconsin for PECAM-1 antibody. The study was supported by funds from the National Institute of Health (AA020098, AA06420 and DA034140 to CDM) and the Veterans Medical Research Foundation start-up funds. TBN was supported by funds from Skaggs School of Pharmacy, UCSD for summer internship.

References

Alikunju S, Abdul Muneer PM, Zhang Y, Szlachetka AM, Haorah J. The inflammatory footprints of alcohol-induced oxidative damage in neurovascular components. Brain Behav Immun. 2011; 25 Suppl 1:S129–136. [PubMed: 21262340]

Arai K, Lo EH. An oligovascular niche: cerebral endothelial cells promote the survival and proliferation of oligodendrocyte precursor cells. J Neurosci. 2009; 29:4351–4355. [PubMed: 19357263]

Coller JK, Hutchinson MR. Implications of central immune signaling caused by drugs of abuse: mechanisms, mediators and new therapeutic approaches for prediction and treatment of drug dependence. Pharmacol Ther. 2012; 134:219–245. [PubMed: 22316499]

Crews FT, Nixon K. Mechanisms of neurodegeneration and regeneration in alcoholism. Alcohol Alcohol. 2009; 44:115–127. [PubMed: 18940959]

Dayer AG, Ford AA, Cleaver KM, Yassaee M, Cameron HA. Short-term and long-term survival of new neurons in the rat dentate gyrus. J Comp Neurol. 2003; 460:563–572. [PubMed: 12717714]

Finnie JW, Manavis J, Chidlow G. Loss of endothelial barrier antigen immunoreactivity as a marker of Clostridium perfringens type D epsilon toxin-induced microvascular damage in rat brain. Journal of comparative pathology. 2014; 151:153–156. [PubMed: 24973988]

Gilpin NW, Richardson HN, Cole M, Koob GF. Vapor inhalation of alcohol in rats. Curr Protoc Neurosci. 2008; Chapter 9 Unit 9 29.

Hansson AC, Nixon K, Rimondini R, Damadzic R, Sommer WH, Eskay R, Crews FT, Heilig M. Long-term suppression of forebrain neurogenesis and loss of neuronal progenitor cells following prolonged alcohol dependence in rats. Int J Neuropsychopharmacol. 2010; 13:583–593. [PubMed: 20334723]

Haorah J, Knipe B, Gorantla S, Zheng J, Persidsky Y. Alcohol-induced blood-brain barrier dysfunction is mediated via inositol 1,4,5-triphosphate receptor (IP3R)-gated intracellular calcium release. J Neurochem. 2007; 100:324–336. [PubMed: 17241155]

Haorah J, Knipe B, Leibhart J, Ghorpade A, Persidsky Y. Alcohol-induced oxidative stress in brain endothelial cells causes blood-brain barrier dysfunction. J Leukoc Biol. 2005; 78:1223–1232. [PubMed: 16204625]

Hernandez JA, Lopez-Sanchez RC, Rendon-Ramirez A. Lipids and Oxidative Stress Associated with Ethanol-Induced Neurological Damage. Oxid Med Cell Longev. 2016; 2016:1543809. [PubMed: 26949445]

Kim A, Mandyam CD. Methamphetamine affects cell proliferation in the medial prefrontal cortex: a new niche for toxicity. Pharmacol Biochem Behav. 2014; 126:90–96. [PubMed: 25260424]

Kim A, Zamora-Martinez ER, Edwards S, Mandyam CD. Structural reorganization of pyramidal neurons in the medial prefrontal cortex of alcohol dependent rats is associated with altered glial plasticity. Brain Struct Funct. 2014

Kim A, Zamora-Martinez ER, Edwards S, Mandyam CD. Structural reorganization of pyramidal neurons in the medial prefrontal cortex of alcohol dependent rats is associated with altered glial plasticity. Brain Struct Funct. 2015; 220:1705–1720. [PubMed: 24667898]

Koob GF, Volkow ND. Neurocircuitry of addiction. Neuropsychopharmacology. 2010; 35:217–238. [PubMed: 19710631]

Lasseter HC, Xie X, Ramirez DR, Fuchs RA. Prefrontal cortical regulation of drug seeking in animal models of drug relapse. Curr Top Behav Neurosci. 2010; 3:101–117. [PubMed: 21161751]

Maki T, Maeda M, Uemura M, Lo EK, Terasaki Y, Liang AC, Shindo A, Choi YK, Taguchi A, Matsuyama T, Takahashi R, Ihara M, Arai K. Potential interactions between pericytes and oligodendrocyte precursor cells in perivascular regions of cerebral white matter. Neurosci Lett. 2015; 597:164–169. [PubMed: 25936593]

Mandyam CD, Harburg GC, Eisch AJ. Determination of key aspects of precursor cell proliferation, cell cycle length and kinetics in the adult mouse subgranular zone. Neuroscience. 2007; 146:108–122. [PubMed: 17307295]

Matsushita T, Lankford KL, Arroyo EJ, Sasaki M, Neyazi M, Radtke C, Kocsis JD. Diffuse and persistent blood-spinal cord barrier disruption after contusive spinal cord injury rapidly recovers following intravenous infusion of bone marrow mesenchymal stem cells. Exp Neurol. 2015; 267:152–164. [PubMed: 25771801]

Miyamoto N, Pham LD, Seo JH, Kim KW, Lo EH, Arai K. Crosstalk between cerebral endothelium and oligodendrocyte. Cell Mol Life Sci. 2014; 71:1055–1066. [PubMed: 24132511]

Newman PJ. The role of PECAM-1 in vascular cell biology. Ann N Y Acad Sci. 1994; 714:165–174. [PubMed: 8017765]

Nixon K, Crews FT. Binge ethanol exposure decreases neurogenesis in adult rat hippocampus. J Neurochem. 2002; 83:1087–1093. [PubMed: 12437579]

Nixon K, Crews FT. Temporally specific burst in cell proliferation increases hippocampal neurogenesis in protracted abstinence from alcohol. J Neurosci. 2004; 24:9714–9722. [PubMed: 15509760]

Park HJ, Shin JY, Kim HN, Oh SH, Song SK, Lee PH. Mesenchymal stem cells stabilize the blood-brain barrier through regulation of astrocytes. Stem cell research & therapy. 2015; 6:187. [PubMed: 26420371]

Pelz J, Hartig W, Weise C, Hobohm C, Schneider D, Krueger M, Kacza J, Michalski D. Endothelial barrier antigen-immunoreactivity is conversely associated with blood-brain barrier dysfunction after embolic stroke in rats. Eur J Histochem. 2013; 57:e38. [PubMed: 24441191]

Phillips C, Baktir MA, Srivatsan M, Salehi A. Neuroprotective effects of physical activity on the brain: a closer look at trophic factor signaling. Front Cell Neurosci. 2014; 8:170. [PubMed: 24999318]

Privratsky JR, Newman DK, Newman PJ. PECAM-1: conflicts of interest in inflammation. Life Sci. 2010; 87:69–82. [PubMed: 20541560]

Richardson HN, Chan SH, Crawford EF, Lee YK, Funk CK, Koob GF, Mandyam CD. Permanent impairment of birth and survival of cortical and hippocampal proliferating cells following excessive drinking during alcohol dependence. Neurobiol Dis. 2009; 36:1–10. [PubMed: 19501165]

Seo JH, Miyamoto N, Hayakawa K, Pham LD, Maki T, Ayata C, Kim KW, Lo EH, Arai K. Oligodendrocyte precursors induce early blood-brain barrier opening after white matter injury. J Clin Invest. 2013; 123:782–786. [PubMed: 23281396]

Somkuwar SS, Fannon-Pavlich MJ, Ghofranian A, Quigley JA, Dutta RR, Galinato MH, Mandyam CD. Wheel running reduces ethanol seeking by increasing neuronal activation and reducing oligodendroglial/neuroinflammatory factors in the medial prefrontal cortex. Brain Behav Immun. 2016; 58:357–368. [PubMed: 27542327]

Somkuwar SS, Fannon MJ, Staples MC, Zamora-Martinez ER, Navarro AI, Kim A, Quigley JA, Edwards S, Mandyam CD. Alcohol dependence-induced regulation of the proliferation and survival of adult brain progenitors is associated with altered BDNF-TrkB signaling. Brain Struct Funct. 2015

Somkuwar SS, Staples MC, Galinato MH, Fannon MJ, Mandyam CD. Role of NG2 expressing cells in addiction: a new approach for an old problem. Frontiers in pharmacology. 2014; 5:279. [PubMed: 25566075]

Souza PS, Goncalves ED, Pedroso GS, Farias HR, Junqueira SC, Marcon R, Tuon T, Cola M, Silveira PC, Santos AR, Calixto JB, Souza CT, de Pinho RA, Dutra RC. Physical Exercise Attenuates Experimental Autoimmune Encephalomyelitis by Inhibiting Peripheral Immune Response and Blood-Brain Barrier Disruption. Mol Neurobiol. 2016

Sternberger NH, Sternberger LA. Blood-brain barrier protein recognized by monoclonal antibody. Proc Natl Acad Sci U S A. 1987; 84:8169–8173. [PubMed: 3500474]

Taupin P. BrdU immunohistochemistry for studying adult neurogenesis: paradigms, pitfalls, limitations, and validation. Brain Res Rev. 2007; 53:198–214. [PubMed: 17020783]

Tiwari V, Kuhad A, Chopra K. Suppression of neuro-inflammatory signaling cascade by tocotrienol can prevent chronic alcohol-induced cognitive dysfunction in rats. Behav Brain Res. 2009; 203:296–303. [PubMed: 19464322]

Vendruscolo LF, Roberts AJ. Operant alcohol self-administration in dependent rats: focus on the vapor model. Alcohol. 2014; 48:277–286. [PubMed: 24290310]

Wang J, Du H, Jiang L, Ma X, de Graaf RA, Behar KL, Mason GF. Oxidation of ethanol in the rat brain and effects associated with chronic ethanol exposure. Proc Natl Acad Sci U S A. 2013; 110:14444–14449. [PubMed: 23940368]

Warthen DM, Lambeth PS, Ottolini M, Shi YT, Barker BS, Gaykema RP, Newmyer BA, Joy-Gaba J, Ohmura Y, Perez-Reyes E, Guler AD, Patel MK, Scott MM. Activation of Pyramidal Neurons in Mouse Medial Prefrontal Cortex Enhances Food-Seeking Behavior While Reducing Impulsivity in the Absence of an Effect on Food Intake. Frontiers in Behavioral Neuroscience. 2016; 10

Westin JE, Lindgren HS, Gardi J, Nyengaard JR, Brundin P, Mohapel P, Cenci MA. Endothelial proliferation and increased blood-brain barrier permeability in the basal ganglia in a rat model of 3,4-dihydroxyphenyl-L-alanine-induced dyskinesia. J Neurosci. 2006; 26:9448–9461. [PubMed: 16971529]

Highlights

- Protracted abstinence from chronic alcohol enhances the proximity of oligodendrocytes with endothelial cells
- Enhanced oligo-vasculature proximity is associated with enhanced blood-brain barrier permeability
- Wheel running during abstinence prevents oligo-vascular maladaptations and normalizes blood-brain barrier permeability

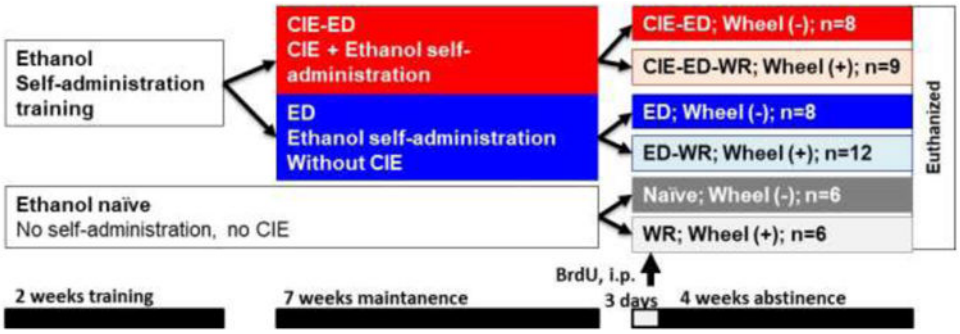

Figure 1.

Schematic of experimental design indicating the experimental groups, the number of animals in each group, time line for each part of the experiment and time point for BrdU injection.

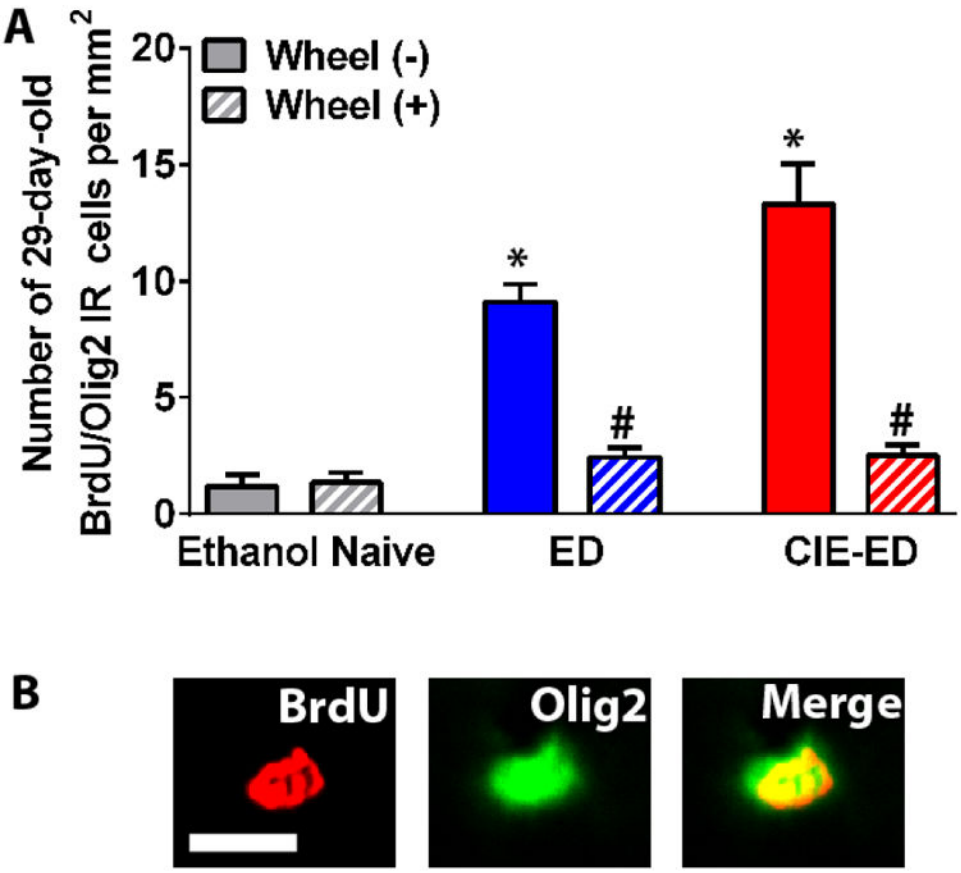

Figure 2.

(a) Quantitative analysis of the number of 28-day-old BrdU/Olig2 colabeled cells in the mPFC. Data is indicated as number of cells per area of the mPFC, and represented as mean ± S.E.M. (b) Representative micrographs for immunofluorescent labeling of 28-day-old BrdU labeled cells colabeled with Olig2 from one control rat. BrdU is in red (CY3) and Olig 2 is in green (FITC). Scale bar indicated in the BrdU panel is 10 μm, applies to all the panels. *p<0.05 vs. ethanol naïve control in nonrunners. #p<0.05 vs. sedentary group in ED and CIE-ED groups. Values are mean ± S.E.M.

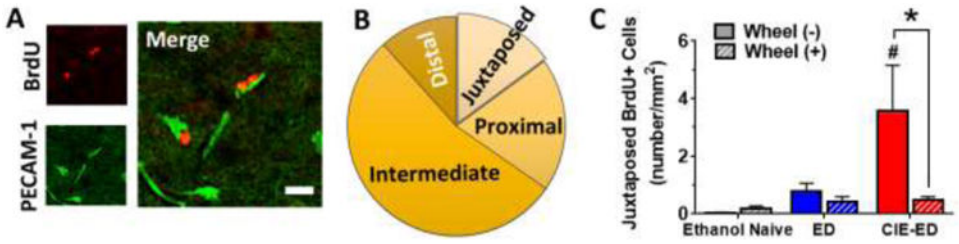

Figure 3.

(a) Representative micrographs for immunofluorescent labeling of 28 day-old BrdU cells (CY3, red) and PECAM-1 (FITC, green) in the mPFC from one CIE-ED rat. Scale bar in the merged panel is 15 μm. (b) Pi-chart presenting the proportion of BrdU+ cells that are juxtaposed, proximal, intermediate or distal from the nearest PECAM-1 labeled cerebral endothelial cells (c) Quantification of the number of BrdU+ cells juxtaposed with cerebral endothelium. #$p<0.05$ vs. ED group; *$p<0.05$ vs. sedentary CIE-ED group.

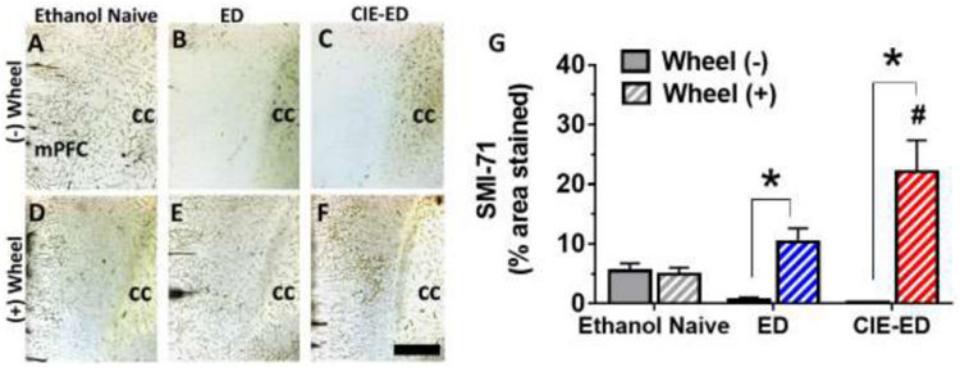

Figure 4.

(a-f) Representative micrographs for immunohistochemical analysis of SMI-71 expression. Scale bar in f is 200 μm, applies a-f. cc, corpus callosum. (g) Quantification of SMI-71 (% area stained). Values are mean ± S.E.M. * $p<0.001$ compared to respective Wheel(-) group; #$p<0.05$ compared to respective ED and ethanol naïve control group.

Table 1

History of ethanol experience increased BrdU+ cells that were at proximal and intermediate distance from PECAM1 in both CIE-ED and ED; both were normalized following wheel access during abstinence. F-statistics from 2-way ANOVAs are presented (F_e, ethanol history, 3 levels; F_w, wheel access, 2 levels; F_i, interaction)

		Ethanol Naïve	ED	CIE-ED	F_e	F_w	F_i
Proximal	Wheel(-)	0.20 ± 0.08	2.3 ± 0.53 #	3.0 ± 0.69 #	8.21 *a*	14.2 *b*	2.87
	Wheel(+)	0.08 ± 0.08	0.73 ± 0.32 *	0.78 ± 0.29 *			
Intermediate	Wheel(-)	0.67 ± 0.41	5.2 ± 0.46 #	5.6 ± 0.89 #	19.9 *a*	39.1 *b*	9.47 *c*
	Wheel(+)	0.80 ± 0.45	1.5 ± 0.26 *	1.8 ± 0.25 *			
Distal	Wheel(-)	0.13 ± 0.09	1.3 ± 0.46	0.97 ± 0.76	1.12	4.91 *b*	1.62
	Wheel(+)	0.26 ± 0.14	0.17 ± 0.09	0.07 ± 0.07			

a p<0.001, significant main effect of ethanol history,

b p<0.05, significant main effect of wheel access,

c p<0.001, significant interaction,

# p<0.05, compared to ethanol naïve control;

* p<0.05, compared to respective Wheel(-)